The Calculation and the Measurement of the Coupling Properties of Dielectric Image Lines of Rectangular Cross Section

KLAUS SOLBACH

Abstract—**In this paper the coupling properties of uniformly coupled dielectric image lines of rectangular cross section are calculated employing an exact method for the determination of the phase constants of the even and the odd mode. The theoretical results are verified experimentally. The results are also applied to the calculation of the coupling characteristics of practical dielectric image line directional couplers.**

I. Introduction

SINCE THE PROPOSAL of the dielectric image line as a guiding structure for millimeter waves, some approximate methods have been proposed for the calculation of the coupling properties of coupled lines [1], [2]. As has been shown by several authors, e.g., Voges [3], the results of the approximate solutions are very inaccurate compared to the experimental results. Yet with respect to the design of directional couplers it is important to calculate the coupling properties of coupled dielectric image lines very accurately. The accuracy of the approximate theory of Marcatili [1] can be improved employing a variational approach on the basis of the approximate solution [3]. In this paper the calculation of the coupling properties is based on the exact solution of the eigenvalue problem of coupled dielectric image lines, published earlier [4].

II. The Method

The cross-sectional view of the uniform coupled dielectric image lines to be discussed here is shown in Fig. 1. Two identical dielectric image guides are spaced by a distance $2(b-w)$ and are covered by an upper shielding plate at a distance d to the ground plane. To avoid the influence of the shielding plate on the coupling properties of the lines, a large value of d was chosen in the calculations. Due to the cross-sectional symmetry of the structure, it is possible to describe the fields of the coupled lines as a superposition of the even and the odd modes. The phase constants β_{even} and β_{odd} are determined employing the method in [4], where the fields of the coupled dielectric image lines of rectangular cross section are calculated by field expansion using the modes of the parallel-plate waveguide.

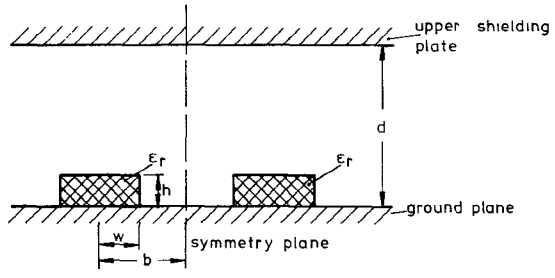

Fig. 1. The cross section of coupled dielectric image lines.

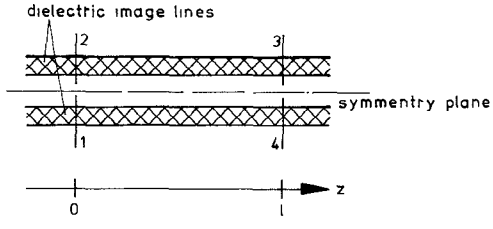

Fig. 2. Uniform coupling section of coupled dielectric image lines.

A wave incident on one of the coupled lines, Fig. 2, due to the difference in the phase constants of the even and the odd modes couples part of its energy to the adjacent line. The length

$$L=\frac{\pi}{\beta_{even}-\beta_{odd}} \tag{1}$$

is needed to transfer the total power of the incident wave to the neighboring line [5]. The scattering coefficients as a function of the length l of the coupling section between the ports, as defined in Fig. 2, can be expressed as

$$|s_{13}|=\left|\sin\left(\frac{\pi}{2}\frac{1}{L}\right)\right| \tag{2}$$

$$|s_{14}|=\left|\cos\left(\frac{\pi}{2}\frac{1}{L}\right)\right|. \tag{3}$$

III. Theoretical Results

The normalized coupling length L/h, where h is the height of the dielectric image guides, was computed from (1) and was plotted in Figs. 3–5 versus the normalized frequency B for a variety of cross-sectional dimensions

Manuscript received May 26, 1978; revised August 10, 1978. This work was supported by the German Research Society (DFG) under Contract Wo 137/4.

The author is with Institut für Allgemeine und Theoretische Elektrotechnik, FB9, Department of Electrical Engineering, University of Duisburg, 41 Duisburg, Germany.

0018-9480/79/0100-0054$00.75 ©1979 IEEE

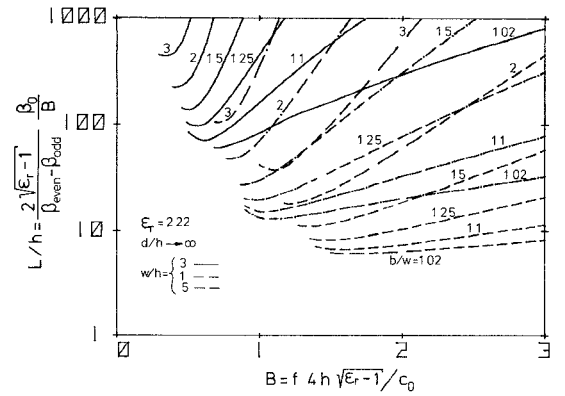

Fig. 3. The normalized coupling length for total power transfer versus the normalized frequency for low-permittivity lines; $w/h \geq 0.5$.

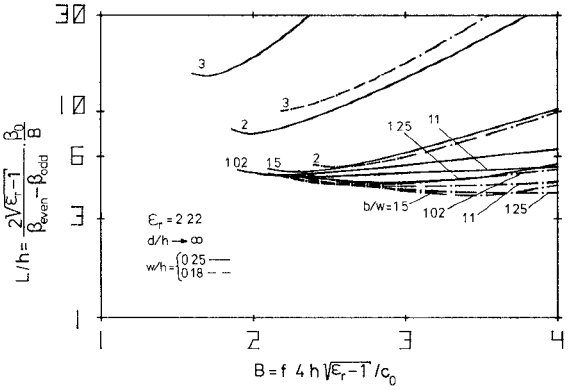

Fig. 4. The normalized coupling length for total power transfer versus the normalized frequency for low-permittivity lines; $w/h < 0.5$.

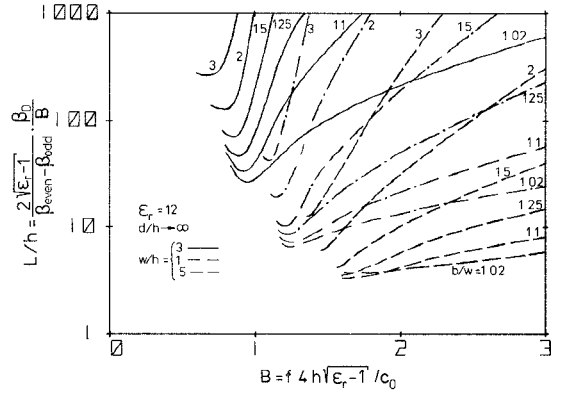

Fig. 5. The normalized coupling length for total power transfer versus the normalized frequency for high-permittivity lines.

and spacings of the guides for low-permittivity lines as well as for high-permittivity lines, where β_0 is the phase constant of plane waves in free space.

From Figs. 3 and 5 it can be concluded that for high normalized frequencies the coupling length versus the normalized frequency approximately is an exponential function and that for lines of high values of the normalized spacing the coupling length approximately increases exponentially with the spacing of the guides. These two dependences have also been calculated using other methods [1]–[3]. Also, in qualitative accordance with these methods it can be concluded from Figs. 3–5 that the normalized coupling length decreases with the aspect ratio of the guides and that the frequency dependence of the normalized coupling length decreases with the aspect ratio. In Fig. 4 the normalized coupling length for lines of very low aspect ratio is plotted versus the normalized frequency. It is obvious that lines of very low aspect ratio, that means lines which are coupled very tightly, exhibit very low frequency dependence of their coupling length L. Employing such lines it should be possible to realize very broad-band directional couplers.

Furthermore, Fig. 4 shows that very tightly coupled dielectric image lines exhibit a minimum coupling length L/h for values of $b/w > 1$. Due to the approximate character of the theories of Marcatili [1] or Toulios and Knox [2] this result cannot be deduced by these methods.

IV. Experimental Verification

The field distribution and the coupling length L of the uniform coupled dielectric image lines of rectangular cross section were experimentally determined using the measurement setup shown in Fig. 6.

The incident wave from the mode launcher propagates along the coupled lines and is absorbed by the matched loads at the end of the lines [7]. In order to reduce reflections and radiation of the incident wave, the transition from the isolated to the coupled image line structure is tapered.

The dielectric image lines were fabricated by a die-casting technique using paraffin wax [6]. The field distribution of the coupled dielectric image lines was probed using a movable electric field probe [7]. In Fig. 7 the measured field distribution is plotted for various transversal planes in the direction of propagation of the waves. It is clearly apparent that the incident wave continuously couples its power to the adjacent guide. At a distance $z = L/2$ from the plane of incidence ($z = 0$) the wave has split into equal parts, whereas at a distance $z = L$ from the plane of incidence the power of the incident wave totally has been coupled to the second guide. The coupling length L was determined by measuring the distances between the planes of maximum and minimum field strength on the lines [3].

In Fig. 8 the results from these measurements are plotted together with the calculated curves for various spacings of the guides. The agreement between the theoretical and the experimental results is good. It is important to mention that the agreement not only is good for high frequencies but also for low frequencies, near the cutoff frequencies of the odd mode. In this frequency range, even the results from the variational approach [3] fail to agree with the measurements.

V. Directional Couplers

Fig. 9 shows sketches of the directional coupler structures which shall be discussed here. The two types of directional couplers only differ in their connecting arms. In the type of Fig. 9(a) coupler, the uniform coupling section has curved connecting guides, whereas in the type

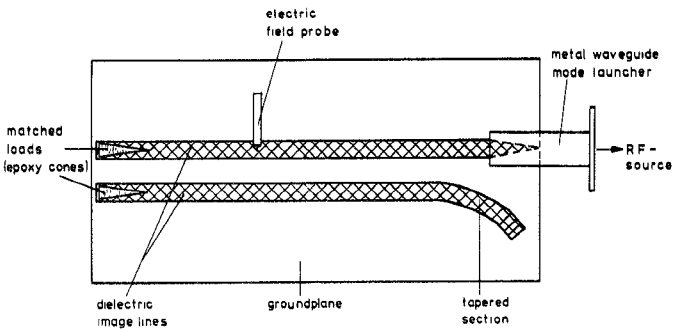

Fig. 6. The measurement setup for the determination of the field distributions of coupled dielectric image lines in the frequency range of 26–40 GHz.

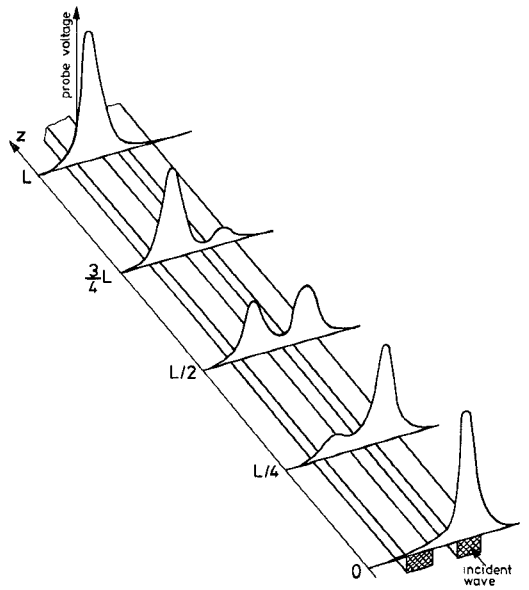

Fig. 7. The field distributions of the waves on coupled dielectric image lines measured in various transversal planes.

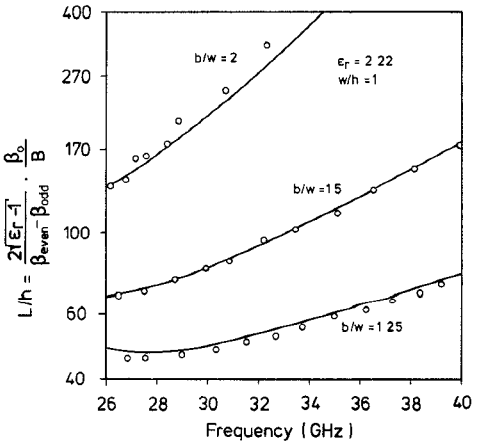

Fig. 8. The coupling length for total power transfer of various coupled dielectric image lines of unit aspect ratio. —— theory; O experimental results.

of Fig. 9(b) coupler, straight lines are used as connecting guides.

As has been demonstrated by Rudokas and Itoh [8] for

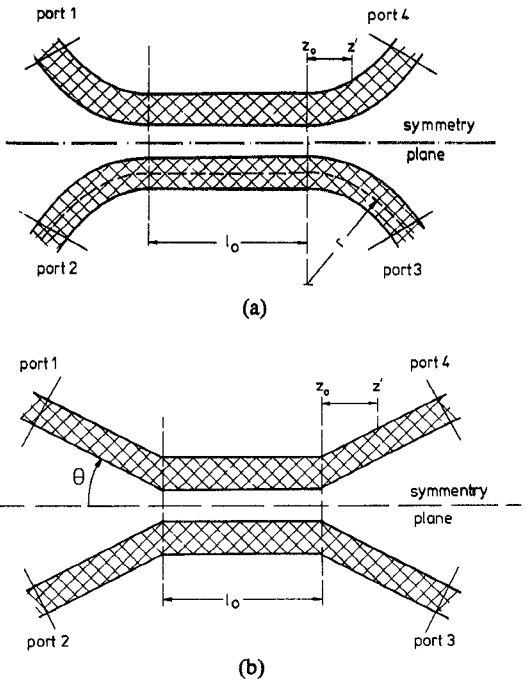

Fig. 9. The directional coupler structures used here incorporating curved (a) and straight (b) connecting arms.

directional couplers made of inverted strip dielectric waveguides, the coupling action of the connecting arms must not be ignored. Thus the scattering coefficients of the directional couplers are calculated analogously to [8] as

$$|s_{13}| = \left|\sin\left(\frac{\pi}{2}\frac{l_{\text{eff}}}{L}\right)\right| \tag{4}$$

$$|s_{14}| = \left|\cos\left(\frac{\pi}{2}\frac{l_{\text{eff}}}{L}\right)\right| \tag{5}$$

where (2) and (3) are modified by the use of the effective coupling length l_{eff}.

Following Rudokas and Itoh, the effective coupling length to a first approximation can be determined from

$$l_{\text{eff}} = l_0 + \frac{2L}{\pi}\int_{z_0}^{z'} (\beta_{\text{even}}(z) - \beta_{\text{odd}}(z))\,dz \tag{6}$$

where the integration is carried out along the axial direction of the directional coupler from the junction z_0 between the uniform coupled line section and the connecting arms to a point z', where the coupling of the connecting arms can be neglected.

In Fig. 10 the scattering coefficients of a directional coupler of Fig. 9(a) are plotted, where both the uniform coupling length l_0 and the effective coupling length l_{eff} were used in the calculations in order to demonstrate the influence of the connecting arms.

In Fig. 11 a photograph of a directional coupler measuring setup is shown. The signal power from an RF source is coupled to the dielectric image line coupler structure through a metal waveguide mode launcher. A second waveguide transition is connected to one of the

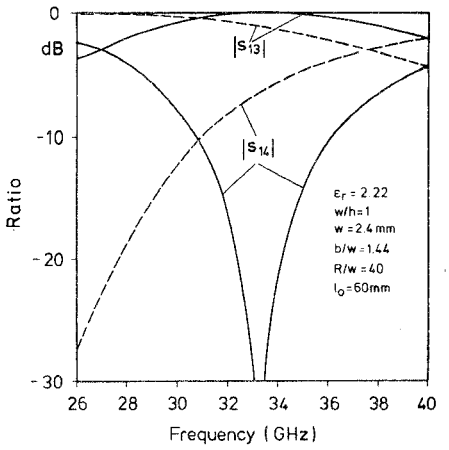

Fig. 10. The theoretical scattering coefficients of Fig. 9(a) directional coupler versus the frequency. —— using l_{eff}; ––– using l_0 in the calculations.

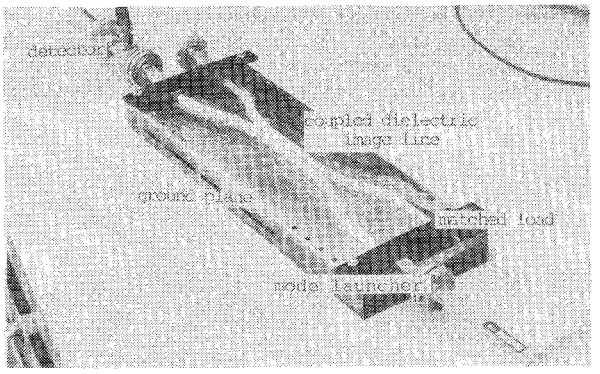

Fig. 11. The measurement setup for the dielectric image line directional couplers. A Fig. 9(a) coupler shown here.

other ports of the coupler, while the remaining arms of the structure are terminated by matched loads [7].

By comparing the output powers from ports 2, 3, and 4, the power ratios P_3/P_4 and P_2/P_3 are determined. From the power ratio P_2/P_3 the scattering coefficients $|s_{12}|$ and $|s_{13}|$ are calculated, assuming the coupler to be lossless. The input reflection coefficient $|s_{11}|$ is determined by measuring the VSWR on the input arm by means of an electric field probe [7].

In Fig. 12 the results of the measurements for a directional coupler of Fig. 9(a) are plotted together with the theoretical curves for $|s_{13}|$ and $|s_{14}|$ using the effective coupling length l_{eff} in the calculations. Considering the approximate nature of the effective coupling length formula (6), the agreement between the theory and the experimental results is reasonable. The poor performance of the directional coupler at about 33 GHz, where $l = L$ should yield ideal isolation of port 4, may be caused by slight asymmetries in the coupler structure. It is interesting to note that the input reflection coefficient $|s_{11}|$ is relatively low and the directivity of the coupler $|s_{12}/s_{13}|$ is high.

In Fig. 13 the results of the measurements for a directional coupler of Fig. 9(b) are plotted together with the

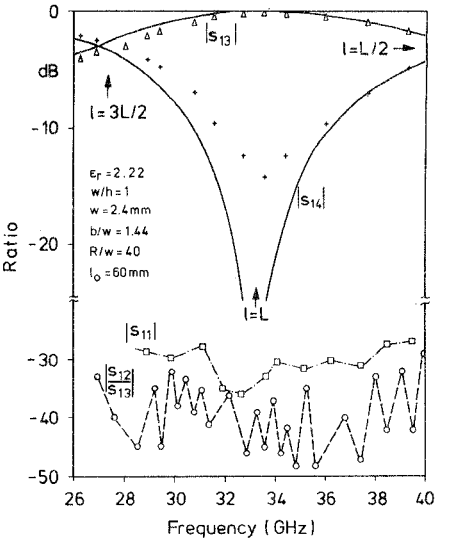

Fig. 12. The scattering coefficients of a Fig. 9(a) coupler versus frequency. —— theory; +, *, O, □ experimental results.

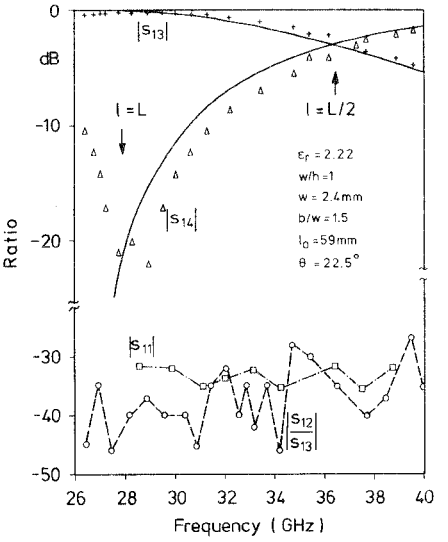

Fig. 13. The scattering coefficients of a Fig. 9(b) coupler versus frequency. —— theory; +, *, O, □ experimental results.

theoretical curves. Comparing Figs. 12 and 13 it can be concluded that the effective coupling length of the Fig. 9(a) coupler is significantly greater than the coupling length of the Fig. 9(b) coupler due to the fact that the curved connecting arms are tightly coupled over a larger distance than the corner shaped connecting lines. It is important to state that the directivity as well as the input reflection coefficient of the Fig. 9(b) coupler are comparable to the values of the Fig. 9(a) coupler. This is surprising since the corner-shaped junctions between the connecting arms and the uniform coupled line section in the Fig. 9(b) coupler form distinct discontinuities of the guiding structure. The insertion loss due to radiation from the junctions was measured in a separate experiment, it was in the range from 3 dB at 27 GHz to 0.9 dB at 40 GHz, while

the input reflection coefficient of the junctions was well below −30 dB in the same frequency range. Thus it can be concluded that the corner shaped junctions in the Fig. 9(b) coupler cause severe radiation losses, while at the same time the low-input reflection and high-directivity values are preserved.

The radiation losses of the curved arms were also measured [9] in a separate experiment and found to be well below 1 dB for frequencies above 27 GHz because of the large curvature radius of the arms.

The overall losses of the dielectric image line directional couplers could not be measured exactly; they range below 2 to 1 dB in the case of the Fig. 9(a) coupler and below 6 to 3 dB in the case of the Fig. 9(b) coupler.

VI. Conclusion

It is shown that it is possible to calculate the coupling properties of uniform coupled dielectric image lines and directional couplers on the basis of dielectric image lines at reasonable accuracy. Some design features for directional coupler structures are also discussed.

References

[1] E. A. Marcatili, "Dielectric rectangular waveguide and directional coupler for integrated optics," *Bell Syst. Tech. J.*, vol. 48, no. 7, pp. 2071–2102, 1969.
[2] R. M. Knox and P. P. Toulios, "Integrated circuits for the millimeter through optical frequency range," in *Symposium on Submillimeter Waves*. New York: Polytechnic Press, 1970, pp. 497–516.
[3] E. Voges, "Directional couplers with rectangular dielectric waveguides," *Arch. Elek. Uebertragungstech.*, vol. 28, no. 11, pp. 478–479, 1974.
[4] K. Solbach and I. Wolff, "The electromagnetic fields and the phase constants of dielectric image lines," *IEEE Trans. Microwave Theory Tech.*, vol. MTT-26, pp. 266–274, Apr. 1978.
[5] S. E. Miller, "Coupled wave theory and waveguide applications," *Bell Syst. Tech. J.*, vol. 33, no. 3, pp. 661–719, May 1954.
[6] K. Solbach, "The fabrication of dielectric image lines using casting resins and the properties of the lines in the millimeter-wave range," *IEEE Trans. Microwave Theory Tech.*, vol. MTT-24, pp. 879–881, Nov. 1976.
[7] ——, "Electric probe measurements on dielectric image lines in the frequency range of 26–90 GHz," *IEEE Trans. Microwave Theory Tech.*, vol. MTT-26, pp. 755–758, Oct. 1978.
[8] R. Rudokas and T. Itoh, "Passive millimeter-wave IC components made of inverted strip dielectric waveguides," *IEEE Trans. Microwave Theory Tech.*, vol. MTT-24, pp. 978–981, Dec. 1976.
[9] K. Solbach, "The measurement of the radiation losses in dielectric image line bends and the calculation of a minimum acceptable curvature radius," this issue, pp. 51–53.

On an Ultrabroad-Band Hybrid Tee

UDO BARABAS

***Abstract*—A hybrid tee is investigated which consists of two broad-band line transformers and a lumped branching point. The branching point forms a bridge circuit, the resistances of which are determined by six lines and their load resistors. The bandwidth is wider than three decades, extending from 2.4 MHz to 5 GHz, and is determined by the transformers. In a special version, the upper cutoff frequency can be shifted to about 12 GHz. The isolation between opposite lines is greater than 40 dB.**

I. Introduction

A HYBRID junction can be defined as a "waveguide arrangement (including coaxial transmission lines), with four branches which, when the branches are properly terminated, has the property that energy can be transferred from any one branch into only two of the remaining three" [1]. In common usage of such junctions, this energy is equally divided between the two branches. Many interesting arrangements of "hybrid tees," as they are also called, have been described. Familiar forms of the hybrid tee for radio frequencies are the magic tee and the hybrid ring, the former consisting of waveguides, the latter being composed of coaxial transmission lines [2]. In a different approach [3], a long gradual taper is required. Good performances over bandwidths exceeding a decade have been obtained. Another approach [4] used a 3-dB asymmetric coupled-transmission-line directional coupler and a Schiffman phase shifter. There, good performance over an octave bandwidth (2–4 GHz) was achieved. Again, another way of realizing hybrid tees is based on 3-dB directional couplers with phase shifters between them [5], [6]. The bandwidth is about four octaves (35–588 GHz) [5] and 8–12 GHz [6], respectively. In a further configuration [7], the hybrid consisted essentially of a coaxial junction with a shielded loop, the axis of which was located at the center of the tee. With such a circuit a bandwidth of approximately 10 percent at about 3 GHz was measured. The isolation between shunt and series arms was in the order of 40 dB. Another rigid coaxial and stripline hybrid tee [8] had a bandwidth of one octave at a frequency of

Manuscript received February 13, 1978; revised July 17, 1978. This work was supported in part by the Deutsche Forschungsgemeinschaft (DFG).

The author is with the Institut für Elektronik, Ruhr-Universität Bochum, D-4630 Bochum, Germany.

0018-9480/79/0100-0058$00.75 ©1979 IEEE